*O*Experimental
ONCOLOGY

EFFECTS OF MECHANOCHEMICALLY ACTIVATED DOXORUBICIN AND 40 MHz FREQUENCY IRRADIATION ON HUMAN A–549 LUNG CARCINOMA CELLS

V.E. Orel[1,]*, Yu.I. Kudryavets[2], S. Satz[3], N.A. Bezdenezhnih[2], M.I. Danko[1],
N.N. Khranovskaya[1], A.V. Romanov[1], N.N. Dzyatkovskaya[1], A.P. Burlaka[2], E.P. Sidorik[2]
[1]Institute of Oncology, Academy of Medical Sciences of Ukraine, Kyiv, Ukraine
[2]R.E. Kavetsky Institute of Experimental Pathology, Oncology and Radiobiology,
National Academy of Sciences of Ukraine, Kyiv, Ukraine
[3]BioNucleonics, Inc., Miami, Florida, USA

Aim: To study *in vitro* influence of mechanochemically activated (MA) doxorubicin (DOXO) and electromagnetic irradiation (EMI) on human lung carcinoma A-549 cells. ***Methods:*** Solid state DOXO was MA by input energy 20 W/g during 5 min. Tumor cells were exposed to 40 MHz EMI with power density 2 W/cm^2 at temperature 37 °C. ***Results:*** Particles of MA DOXO have sizes 10 time smaller than officinal DOXO, high performance liquid chromatography analysis showed that parameters of officinal and MA DOXO were quantitatively equal. Mechanochemical activation initiated in the drug formation of free radicals with g = 2.005, g = 2.003 and g = 1.97. LD$_{50}$ values of MA DOXO were 5 times lower than that of officinal drug. Cell survival decreased in the following way after effects EMI → officinal DOXO → MA DOXO → officinal DOXO + EMI → MA DOXO + EMI. ***Conclusion:*** Treatment by MA DOXO and drug with EMI at 37 ºC showed better targeting of drug in human lung carcinoma A-549 cells outcomes than officinal DOXO.
Key Words: A-549 human lung carcinoma cells, doxorubicin, mechanochemical activation, electromagnetic irradiation.

Doxorubicin (DOXO) is an anthracycline quinone antineoplastic antibiotic that has been shown to have activity against a variety of solid human tumors. The mechanisms of DOXO–induced cytotoxicity have been extensively studied and have been shown to include free radical formation and absorption of DOXO into the double helix of DNA resulting in topoisomerase II–mediated DNA damage [1–3]. DOXO also causes depolarization of the membrane lipid bilayer in different cancer cell lines [4].

It is known that exposure to the electromagnetic fields causes depolarization of cell membranes and modifies drug resistance of tumor cells [5, 6]. In several studies DOXO was combined with electromagnetic induced hyperthermia to enhance the efficacy of the drug. However, elevated temperatures caused the increased cytotoxicity of this antitumor agent as shown *in vitro* and *in vivo* [7].

Recently, novel technologies for producing drugs suitable for delivery in the form of micro and nanoparticles have been developed [8]. Specifically, one such technology, known as mechanochemical activation, applies friction and impact energy to drug molecules during grinding.

Results in one preclinical trial employing mechanochemically activated (MA) drugs have demonstrated an increased therapeutic efficacy [9].

Previously, our group has shown that while the primary chemical structure of MA DOXO remained unaltered, the concentration of monovalent and divalent

positively charged ions of the drug increased [10]. This paper examines the effect of MA DOXO and electromagnetic irradiation (EMI) for targeting *in vitro* human A–549 lung carcinoma cells.

MATERIALS AND METHODS

Cell culture conditions. Human A–549 lung carcinoma cell line obtained from the Cell Bank of the R.E. Kavetsky Institute of Experimental Pathology, Oncology and Radiobiology of National Academy of Sciences of Ukraine (Kyiv, Ukraine) was used. Cells were cultured in RPMI–1640 medium (Sigma, USA) with 10% fetal calf serum (Sangva, Ukraine), 2 mM L–glutamine (Gibco, USA), 100 U/ml penicillin and 100 µg/ml streptomycin (referred to as complete medium). Cells were cultured in humidified air containing 5% CO$_2$ at 37 °C, and were routinely replenished every 4 days in medium by seeding 2–3 × 10^4 cells/cm^2. In experiments, cells in an exponential phase of growth were used.

Mechanochemical activation. Lyophilized DOXO (Pharmacia & Upjohn) was MA in an MMVE–0.05 microvibromill (GEFEST, Russia). The micronized powder (10 mg) was placed in a chamber with 5 grinding spheres. Mechanical processing was performed at a frequency of 50 Hz at an amplitude of 9 mm for 5 min. Officinal (OF) DOXO was micronized using an input energy of 20 W/g for 5 min. MA DOXO particles produced are 10 times smaller than OF DOXO.

Electromagnetic irradiation. Petri dishes containing A–549 cells were exposed to 40 MHz electromagnetic field at a power density of 2 W/cm^2. The calculated electric field was 27.5 V/m and the magnetic field was 22 A/m. Cells were exposed inside a 3 cm diameter round irradiation frame [11].

Treatment of cells, estimation of survival and inhibition of proliferation. A–549 cancer cells were seeded in 24–well tissue culture plates (3×10^4 cell per well), or into 30 mm diameter Petri dishes (2×10^5 cells per dish) and cultured in complete medium at 37 °C with various DOXO concentrations. After 48 h incubation with drugs cells were counted and viability was assessed by Trypan blue dye exclusion testing.

To test the combined action of DOXO and EMI the drug was added to the cells in Petri dishes for 100 min, and the plates were irradiated for 30 min at 40 MHz.

Electron microscopy measurements. Observation was performed at 15 kV by scanning raster electron microscopy using a Cam Scan S–4 (UK) at secondary electron emission. DOXO was placed onto a carbon film.

High performance liquid chromatography. Analytical equipment for a Shimadzu HPLC model LC–10ADvp Shimadzu HPLC 10 Dvp system (LC–10ADvp intelligent pump coupled to a SIL–10ADvp autosampler and SPD–M10Avp UV/VIS detector) for high performance liquid chromatograph (HPLC) analyses coupled to a CC Nucleosil 100–5 C18 HD column (0.4×25 cm, Machinery-Nagel, Du¨ren, Germany). The solvent system was acetonitrile: 39 mM NaH_2PO_4 buffer (pH = 2.5), isocratic gradient: 30% acetonitrile: 70% buffer, 1 ml/min flow rate, with detection at 249 nm [12].

Electron spin resonance (ESR) spectroscopy. ESR spectra of MA DOXO were recorded on an RE–1307 spectrometer (Russia) at the temperature of liquid nitrogen (77K).

Fractal dimension analysis. Irregularities common to tumor cell shapes and structures are often characterized as chaotic and quantified by a single descriptive parameter known as the fractal dimension (FD). Nonsymmetrical irregular structures (chaos) in tumor cells were determined by FD analysis from digital images using the box–counting method [13, 14]. In order to achieve this, phase contrast photographs of A–549 tumor cells were taken. The film was processed according to Frieser [15]. Then the negative images were scanned at 4,000 dpi (Nikon 8000 scanner, Japan) and inputted into a personal computer as a two–dimensional data set. The obtained data was further processed and diagrams of optical density were plotted.

Flow cytometry. Flow cytometry analysis was performed on a FACScan (Becton Dickinson, USA) and an argon laser using CellQuest analysis software for Mackintosh computers. Excitation at 488 nm and 585 nm and a band pass filter (bandwidth 42 nm) was used for obtaining red fluorescence given rise to from propidium iodide staining of DNA.

After incubation cells were washed and fixed in cold ethanol at 70 °C. Cells ($1 \times l0^6$) were then washed in phosphate buffered saline and resuspended in 1 ml of hypotonic lysis buffer (0.1% sodium citrate, 0.1% Triton X–100, 5 µg/ml propidium iodide (Sigma, USA)). 250 µg/ml of RNAse type A was added to cell samples. After gentle mixing the cells were incubated at 22–25 °C for 30 min in darkness.

Apoptosis levels and cell–cycle phase distribution were determined by flow cytometry after propidium iodide staining of cells. The leakage of fragmented DNA from apoptotic nuclei was measured using the technique of Nicoletti et al. [16] with modifications.

Cell cycle histograms were analyzed by ModFit LT2.0 flow cytometric software for Mackintosh computers [17].

Statistical procedures. Data obtained were analyzed by Student's *t*–test. 5–10 samples were measured in each experiment. Nonlinear kinetics of the tumor cells survival after DOXO treatment was described by exponential regression curves using a Microsoft Excel:

$$y = b \cdot exp(-kx), \tag{1}$$

where *y* is the survival of A–549 cells; *x* is the concentration of DOXO, and *b* and *k* are regression parameters.

RESULTS

Electron microscopy measurements. Electron microscopy (Fig. 1) has shown that MA DOXO particles ranging from 1–10 µm have more chaotic particle shapes as determined by electron microscopy measurements. The sizes of OF DOXO particles are 10–100 µm.

HPLC analysis. An HPLC chromatogram and UV–VIS spectrum for OF and MA DOXO in solution is shown in Fig. 2. The retention times (5.3 min) and UV–VIS spectra for both compounds are identical. After a column was loaded, both substances registered similar peaks. The greatest light absorbance peaks were at 233, 253, 291, 477, 481 and 531 nm. The UV spectrum of the peak registered at 7.4 min differed from the spectrum of aglycone and represents an impurity.
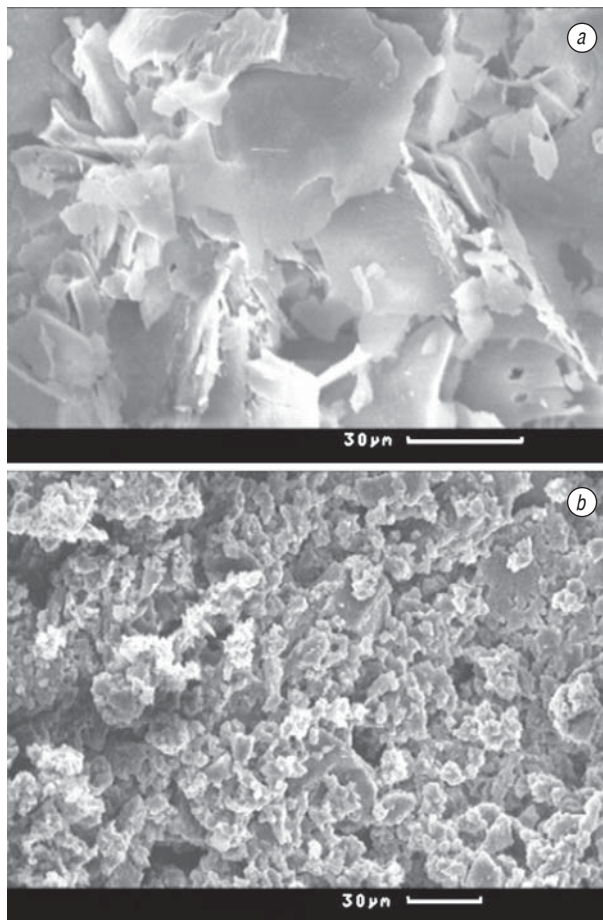
Fig. 1. Microstructure of DOXO observed by scanning raster electron microscope: *a* — OF DOXO; *b* — MA DOXO
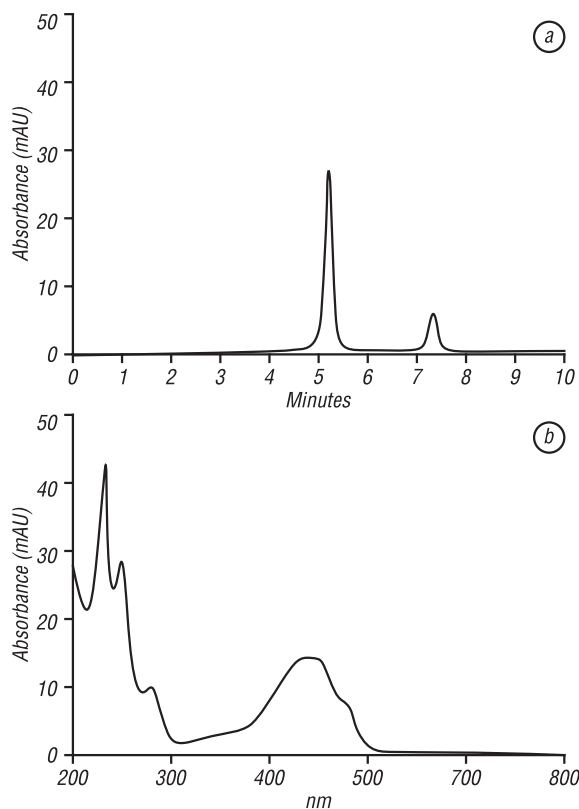
Fig. 2. HLPC chromatogram (a) and spectrum UV–VIS (b) for OF and MA DOXO. Concentration 0.2 mg/ml, injection volume 5 µl

ESR Measurements. Mechanochemical activation of DOXO (Table 1) resulted in free radical formation with g = 2.005; g = 2.003; g = 1.97 (Fig. 3, Table 1).
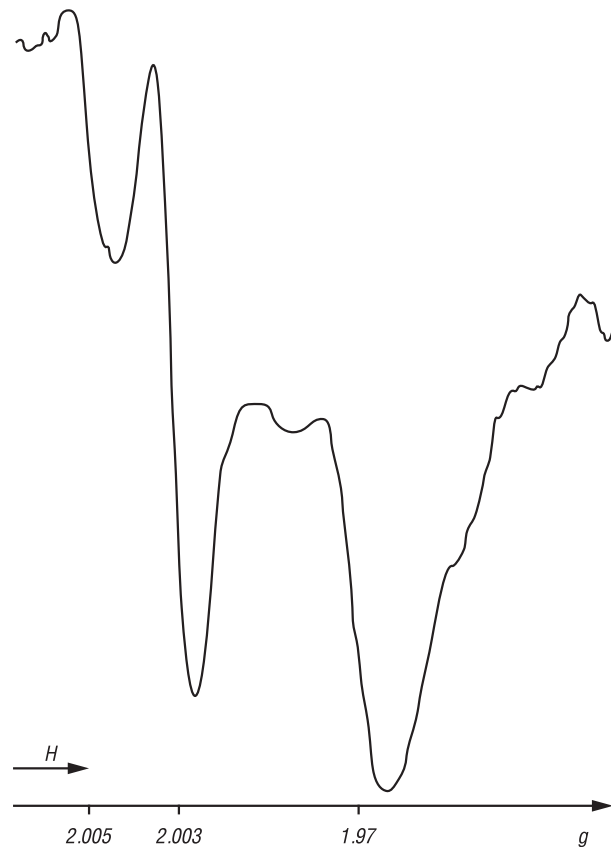
Fig. 3. The electron spin resonance spectrum of MA DOXO (4 mg/ml). Technical characteristics: analytical sensitivity 10^{15} spin/T; power 200 mW; modulation frequency 100 кHz; standard — ions Mn^{2+} in crystal lattice of MgO ($2.68 \cdot 10^{15}$ spin/mg)

Table 1. Change in spin concentration of free radicals (C, 10^{15}/mg) in MA DOXO and official DOXO

MA DOXO	OF DOXO	g-factor
515	103	1.97
845	185.5	2.003
361	155	2.005

Cytotoxicity and FD analysis. A comparison of cytotoxic and antiproliferative effects of OF DOXO and MA DOXO in A–549 cancer cells is shown in Fig. 4. Experimental data are approximated by exponential function in accordance with the equation (1) $y = 20.1 \exp(-0.18\,x)$ for OF DOXO and $y = 27.1 \exp(-0.17\,x)$ for MA DOXO.
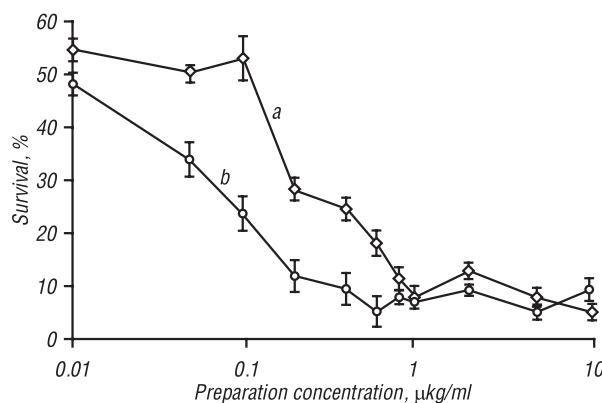
Fig. 4. Cytotoxic effect of DOXO in A–549 cells OF (a) and MA (b) DOXO

Based upon experiments in A–549 cancer cells using 24 well plates comparing OF DOXO and MA DOXO, the potential antineoplastic effect of MA DOXO exceeded that OF DOXO by 80% (LD_{50} is 0.05 µg/ml for OF DOXO and 0.01 µg/ml for MA DOXO).

Fig. 5 shows images of intact A–549 cells as well as cells treated with MA and OF DOXO. According to fractal analysis data, the maximum FD corresponds to untreated cancer cells (Table 2). The decrease of FD for tumor cells structures is observed after treatment by DOXO. A–549 cancer cells damaged by DOXO have transformed from a generally chaotic state to more spherical. Minimum FD corresponds to cell structures after treatment by MA DOXO.

Table 2. Fractal dimensions of A–549 cells without treatment (control) and treated with 0.2 µg/ml doxorubicin

Treatment	Fractal dimension (n = 20)
None	1.848 ± 0.023
OF DOXO	1.621 ± 0.081
MA DOXO	1.419 ± 0.037

Inhibition of proliferation. Results of growth inhibition in A–549 cancer cells from different treatment modes are given in Fig. 6. In this experiment cells were grown in 30 mm Petri dishes. EMI alone demonstrated 23.5% reduction of cell proliferation ($p < 0.05$). Exposure to MA DOXO at final concentration of 0.1 or 0.2 µg/ml for 48 h inhibited the proliferation of A–549 cancer cells more than OF DOXO. Different treatment modes have been compared and the effect of cell proliferation inhibition were shown to increase in the following order: EMI < OF DOXO < MA DOXO < OF DOXO with EMI < MA DOXO with EMI. The additional antiproliferative effects of combination DOXO and EMI are presented. It should also be noted that the effects observed
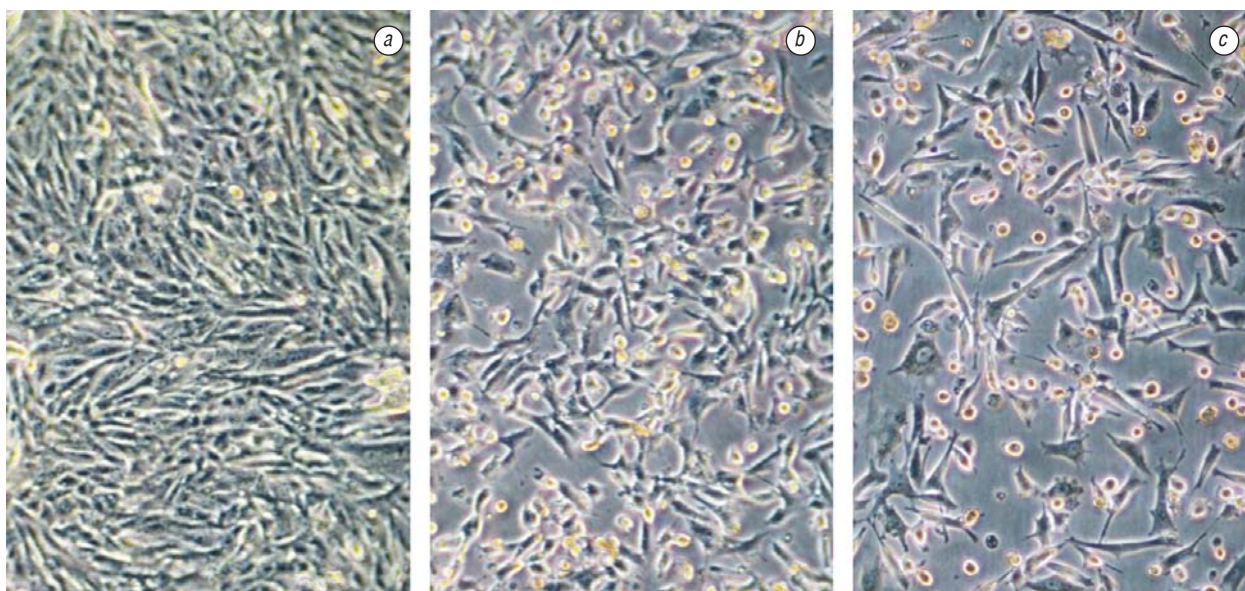
Fig. 5. A–549 cancer cells without treatment (control) (*a*) and treated by OF (*b*) and MA DOXO (*c*) 0.2 µg/ml (magnification x 20)
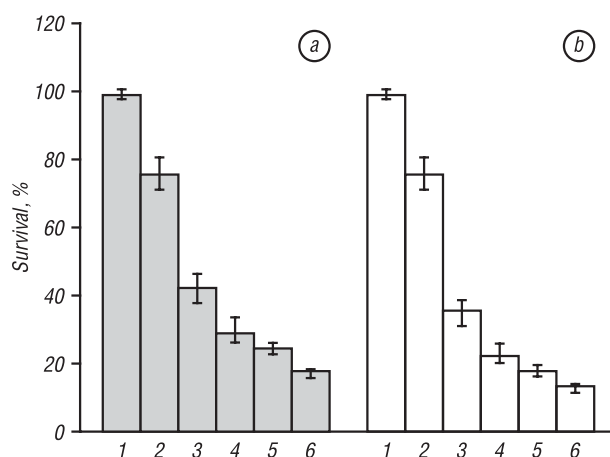
Fig. 6. Growth inhibition effect of DOXO and EMI in A–549 cells: *a* — OF DOXO; *b* — MA DOXO: *1* — without treatment (control); *2* — EMI; *3* — OF DOXO; *4* — MA DOXO; *5* — OF DOXO with EMI; *6* — MA DOXO with EMI. Drug concentration: *a* — 0.1 µg/ml; *b* — 0.2 µg/ml

in this study generally appear to be cytostatic since the percentage of the dead cells in the exposed cell populations did not exceed 5–7%.

Apoptosis induction. These data summarized in Table 3 show the effect of different modes of treatment on apoptosis in A–549 cells. Flow cytometry of A–549 cancer cells exposed to EMI demonstrates that EMI alone results in only a slight increase in apoptosis (no more than 5%) as compared with intact A–549 cells. At the same time, the percentage of apoptotic cells after incubation with OF DOXO for 48 h at the doses of 0.1 and 0.2 µg/ml was 22.2% and 24.3%, respectively, while exposure to MA DOXO increased the apoptotic percentage by only 2.3% when compared with OF DOXO. Combined treatment with EMI with OF DOXO (0.1 µg/ml) results in an increase in apoptosis of as much as 37.9%. Similarly, increased apoptosis from combined therapy of DOXO and EMI was observed at a DOXO dose of 0.1 µg/ml. However, the increase of DOXO dose with aim to enhance the apoptosis–inducing effects of combined EMI with OF DOXO appears to be less pro-

nounced. Moreover, combined treatment using EMI with MA DOXO did not result in a significant increase in apoptosis when compared with MA DOXO alone at drug concentrations of 0.1 µg/ml and 0.2 µg/ml.

Cell cycle distribution. Fig. 7 shows the patterns of cell cycle distribution using the aforementioned modes of the treatment. These data are also summarized in Table 3. While the percentage of S–phase cells varied in different DOXO treatment modes studied (untreated cells, OF DOXO, MA DOXO) from 18.4% in intact cells up to 47.9% in MA DOXO–treated cells, in each of these treatment modes, except for OF DOXO, the corresponding S–phase cell percentage was not affected significantly by EMI. Therefore, EMI alone did not result in further redistribution of DOXO–treated or untreated cells
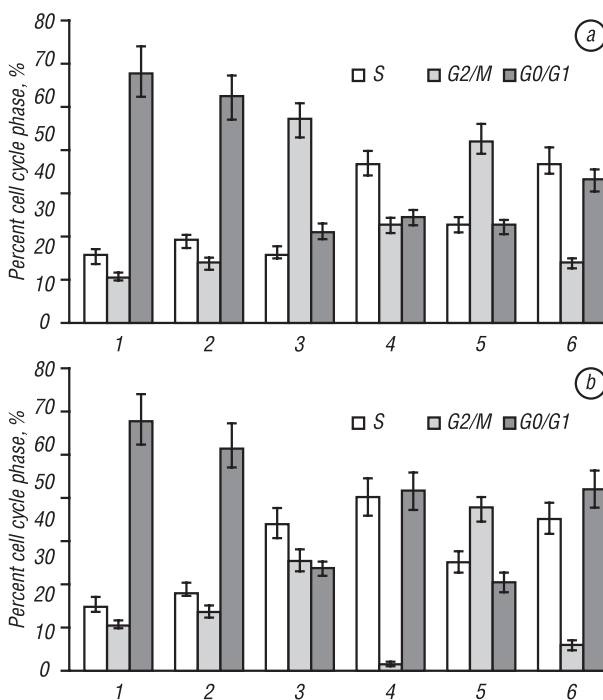
Fig. 7. DOXO and EMI–induced changes in cell cycle distribution for A–549 cancer cells: *1* — without treatment (control); *2* — EMI; *3* — OF DOXO; *4* — MA DOXO; *5* — OF DOXO with EMI; *6* — MA DOXO with EMI. Drug concentration: *a* — 0.1 µg/ml; *b* — 0.2 µg/ml

Table 3. Cell cycle distribution and apoptosis in A–549 cells exposed to OF DOXO, MA DOXO, EMI and combinations

№	Treatment modality	Cell cycle distribution (%)			Apoptotic (%)
		Cell cycle stages			
		G0/G1	S	G2/M	
1	Untreated cells	68.64	18.41	12.95	14.63
2	EMI	61.16	22.23	16.61	19.84
3	OF DOXO (0.1 µg/ml)	25.08	19.59	55.53	22.16
4	OF DOXO (0.1 µg/ml) with EMI	26.48	27.22	50.39	37.86
5	MA DOXO (0.1 µg/ml)	29.12	43.89	27.0	24.46
6	MA DOXO (0.1 µg/ml) with EMI	39.2	44.22	16.59	25.91
7	OF DOXO (0.2 µg/ml)	28.44	40.86	30.7	24.28
8	OF DOXO (0.2 µg/ml) with EMI	24.97	30.17	44.86	31.27
9	MA DOXO (0.2 µg/ml)	49.46	47.88	2.66	26.64
10	MA DOXO (0.2 µg/ml) with EMI	50.23	42.10	7.67	27.00

according to the cell cycle phases. A substantial accu–mulation of cells in a G2/M phase was found, especially after exposure to OF DOXO and OF DOXO with EMI at a dose level of 0.1 µg/ml. As the DOXO concentration increases, distribution in accordance with the cell cycle phases shifts towards S and G0/G1 phases.

DISCUSSION

Electron microscopy measurements indicate that MA DOXO particles are 10 times smaller than OF DOXO. Decreased particle size increases its solubility and reactivity [19].

HPLC analysis confirms that the chromatographic characteristics of OF and MA DOXO are identical. This suggests the possibility of using a OF standard com–pendial protocol (i.e., US Pharmacopoeia or BP) for MA DOXO purity testing.

Analysis of ESR DOXO spectra testifies that mecha–nochemically activated DOXO initiated free radicals formation with g = 2.005, g = 2.003 and g = 1.97. Ear–lier, OF DOXO has been studied in [18]. Most likely, this is the result of a defect formation of DOXO struc–ture due to mechanical activation [19]. Free radicals produced self–assembling microparticles in solid states of drug and are disintegrated into nanoparticles after solution. The concentration of monovalent and diva–lent positively charged ions of the drug increased [10]. Since the free–radical mechanism seems to be involved in DOXO–triggered tumor cell damage [20, 21], the in–creasing free radicals formation in MA DOXO may re–sult in an enhancement of the antineoplastic effect of MA DOXO as compared to OF DOXO.

Proliferation of A–549 cells treated with MA DOXO or OF DOXO suggest enhanced cytotoxicity of MA DOXO as compared with identical doses of the OF form of the drug. It was also established by fractal analysis that MA DOXO results in a less pronounced chaotic structural organization of A–549 cells compared with the effects of the OF form of this drug. Observed mor–phological effects were likely to result from determinis–tic nonlinear regulatory mechanisms influenced by an anticancer treatment regimen [22].

EMI alone inhibited A–549 cells growth by up to 23.5%. A combination of DOXO and EMI substantially inhibited cancer cell proliferation when compared with DOXO alone (up to 82%). The reverse effect was ob–served in apoptosis rate of A–549 cell. EMI alone initiat–ed a slight (5%) increase in the hypodiploid cell number

in comparison with control cells, combination of OF DOXO and EMI increased the apoptotic rate as com–pared to OF and MA DOXO. Combined EMI with OF DOXO (0.1 µg/ml) results in increased apoptosis (up to 37.9%), suggesting the potential benefit of such a com–bination, and the same holds true after assessing cyto–toxicity of the aforementioned combined treatment. Nev–ertheless, increasing the dosage of the drug (0.2 µg/ml) appears to balance out these observed antiproliferative and proapoptotic effects, probably due to mitotic cycle distributions of cancer cells when the cells differ in terms of sensitivity to the chemotherapeutic cytotoxic or apo–ptotic action. The same is evident when comparing the percentage of cells undergoing apoptosis in MA DOXO and MA DOXO with EMI treatment in which there are pronounced differences in the number of the cells count–ed in these two modes. This may have resulted from the nonlinear nature of combination therapy using different drug forms and EMI [5, 23]. Such a discrepancy bet–ween the effects accounted for by two different ap–proaches should be taken into consideration in further studies on the antiproliferative and the proapoptotic ef–fects of different treatment modalities.

Depending upon the cell cycle phase, the data on cell distribution demonstrates cell delay in the G2/M phase as the initial manifestation of the cytotoxicity. In–crease of the drug dose resulted in enhanced cytotoxic–ity accompanied by an accruing blockage with accu–mulation of the cells in S and subsequently — in G0/G1 phases. Maximum cytotoxicity is achieved using MA DOXO at the dose of 0.2 µg/ml and MA DOXO with EMI. The number of A549 cancer cells entering the G2/M phase decreased notably (3–7% *vs*. 13–15% in the untreated cell population) with the remainder of the cells in the G0/G1 (50%) and S–phases (42–48%).

EMI has a slight influence on the cell population structure in comparison with the control cells without treatment. The most significant inhibition of cell prolife–ration in the S–phase was found in experiments using MA DOXO. This confirms a decrease in DNA synthe–sis resulting from MA DOXO action in experiments on A–549 cells [24].

While the molecular mechanisms of MA DOXO bind–ing are not fully understood, unlike OF DOXO, MA DOXO, with their smaller volume of distribution, charge charac–teristics and kinetics of uptake are preferentially taken up into cancer cells. For given amounts of intracellular DOXO, the encapsulated form of the drug (i.e., hyaluronan–tar–geted liposomes) was more potent and efficient than the free drug. The outcome was expressed in the kinetic model as a larger rate constant of cell killing potency for the en–capsulated drug *versus* the free drug [25]. This model provides a quantitative framework for comparing the cy–totoxic effect in cultured cells when applying the drug in the free form or in a delivery system. The physical and chemical processes underlying enhanced anticancer ef–fect resulted from its mechanochemical activation and mi–cronization coupled with 40MHz EMI needs to be further elucidated. In particular, data on EMI interaction with cell receptors [26–28] suggested that the physico–chemical

mechanism of EMI potentiation of DOXO antineoplastic effects at physiological temperatures may be connected with the initiation of membrane depolarization due to radical states induced by mechanochemical drug activation. All these effects may contribute to an inhibition of DNA synthesis and DNA topoisomerase II activity and linkage with this enzyme and its transformation to a DNA–damaging agent, the so–called "cleavable complex". Also, interference between DNA bases pair is intensified resulting in damage of cell structures and the initiation of apoptosis [29, 30], all these effects appear to vary with the drug dose in a nonlinear fashion. Thus, one may conclude that there is an increased antineoplastic effect of MA DOXO on A–549 cells when compared with OF DOXO at identical doses and an even greater DOXO anticancer effect as a result of the combined action of the drug and 40 MHz EMI at 37 °C. The aforementioned effects may find pragmatic applications in clinical practice for tumor cell targeting.

ACKNOWLEDGEMENTS

REFERENCES

1. **Bachur NB.** Anthracycline antibiotic pharmacology and metabolism. Cancer Treat Rep 1979; **63**: 81725.

2. **Reszka KJ, Mc Cormick ML, Britigan BE.** Peroxidase- and nitrite-dependent metabolism of the anthracycline anticancer agents daunorubicin and doxorubicin. Biochemistry 2001; **40**: 15349–61.

3. **Shao J, DeHaven J, Lamm D, Runyan K, Malanga CJ, Rojanasakul Y, Ma JKH.** A cell-based drug delivery system for lung targeting: 1. Preparation and pharmacokinetics. Drug Delivery 2001; **8**: 61–9.

4. **Pacilio C, Florio S, Pagnini U, Crispino A, Claudio PP, Pacilio G, Pagnini G.** Modification of membrane fluidity and depolarization by some anthracyclines in different cells lines. Anticancer Res 1998; **18**: 4027–34.

5. **Hirata M, Kusuzaki K, Takeshita H, Hashiguchi S, Hirasawa Y, Ashichara T.** Drug resistance modification using electromagnetic field stimulation for multidrug resistant mouse osteosarcoma cell line. Anticancer Res 2001; **21**: 317–32.

6. **Pasquinelli P, Petrini M, Mattii L, Galimberti S, Saviozzi M, Malvaldi G.** Biological effects of PEMF (pulsing electromagnetic field): an attempt to modify cell resistance to anticancer agents. J Environ Pathol Toxicol Oncol 1993; **12**:193–7.

7. **Marmor JB.** Interactions of hyperthermia and chemotherapy in animals. Cancer Res 1979; **39**: 2269–76.

8. **Au JL, Jang SH, Zheng J, Chen C, Song SHL, Wientjes MG.** Determinants of drug delivery and transport to solid tumors. J Control Release 2001; **74**: 31–46.

9. **Kondo SA.** Design and development of novel polymeric prodrugs prepared by mechanochemical solid-state polymerization. Yakugaku Zasshi 2000; **120**: 1337–46.

10. **Todor IN, Orel VE, Mikhailenko VM, Danko MI, Dzyatkovskaya NN.** Influence of mechanochemically modified doxorubicin and irradiation with frequency 40 MHz on doxorubicin-resistant Guerin's carcinoma. Exp Oncol 2002; **24**: 234–6.

11. **Medinets YuR, Orlovskiy AA.** Magnetothermia — therapeutic heating in magnetic field of high frequency. Med Physics 2003; **17**: 67–74 (In Russian).

12. The United States Pharmacopoeia The National Formulary. USP XXII NF XVII. United States Pharmacopeial Convention, 1990; INC: 478.

13. **Losa GA.** Fractal in pathology: are they really useful? Pathologica 1995; **87**: 310–7.

14. **Losa GA.** Fractal morphometry of cell complexity. Rev Biol 2002; **95**: 239–58.

15. **Frieser H.** Photographic information recording. London: Focal Press, 1975; 237 p.

16. **Nicoletti I, Migliorati G, Pagliacci MC, Grignani F, Riccardi C.** A rapid and simple method for measuring thymocyte apoptosis by propidium iodide staining and flow cytometry. J Immunol Meth 1991; **139**: 271–9.

17. **Merkel DE, Mc Guire WL.** Ploidy, proliferative activity and prognosis: DNA flow cytometry of solid tumors. Cancer 1990; **65**: 1194–205.

18. **Mimnaugh EG, Kennedy KA, Trush MA, Sinha BK.** Adriamycin-enhanced membrane lipid peroxidation in isolated rat nuclei. Cancer Res 1985; **45**: 3296–304.

19. **Heinike G.** Tribochemistry. Berlin: Akademia-Verlag, 1984.

20. **Kalinina YeV, Saprin AN, Solomka VS, Sherbak NP, Piruzyan LA.** Inhibition of hydrogen peroxide, oxygen and semiquione radicals in the course of formation of resistance of human erytroleukemia K562 cells to doxorubicin. Problems Oncol 2003; **49**: 294–8.

21. **Praet M, Calderon PB, Pollakis G, Roberfroid M, Ruysschaert JM.** A new class of free radical scavengers reducing adriamycin mitochondrial toxicity. Biochem Pharmacol 1988; **37**: 4617–22.

22. **Ahammer H, Devaney TTJ, Tritthart HA.** Fractal dimension for a cancer invasion model. Fractals 2001; **9**: 61–76.

23. **Rudge S, Peterson C, Vessely C, Koda J, Stevens S, Catterall L.** Adsorption and desorption of chemotherapeutic drugs from a magnetically targeted carrier (MTC). J Control Release 2001; **74**: 335–40.

24. **Studzian K, Wasowska M, Piestrzenieicz MK, Wilmanska D, Szmigiero L, Oszczapowicz I, Giniazddowski M.** Inhibition of RNA synthesis *in vitro* and cell growth by anthracycline antibiotics. Neoplasma 2001; **48**: 412–8.

25. **Eliaz E, Rom N, Shlomo MC, Szoka FC.** Determination and modeling of kinetics of cancer cell killing by doxorubicin and doxorubicin encapsulated in targeted liposomes. Cancer Res 2004; **64**: 711–8.

26. **Bezrukov SM, Vodyanoy I.** Signal transduction across alamethicin ion channels in the presence of noise. Biophys J 1997; **73**: 2456–64.

27. **Blanchard JP, Blackman CF.** Clarification and application of an ion paramagnetic resonance model for magnetic field interactions with biological resonance systems. Bioelectromagnetics 1994; **15**: 217–38.

28. **Liboff AR.** Cyclotron resonance in membrane transport. In: Interaction between electromagnetic field and cells. Chiabrera A, Nicolini C, Schwan HP, eds. New York: Plenum, 1985: 281–96.

29. **Hortobagyi GN.** Anthracyclines in the treatment of cancer. Drugs 1997; **54**: 1–14.

30. **Patel S, Sprung AU, Keller BA., Heaton VJ, Fisher LM.** Identification of yeast DNA topoisomerase II mutants resistant to the antitumor drug doxorubicin: implications for the mechanisms of doxorubicin action and cytotoxicity. Mol Pharmacol 1997; **52**: 658–66.

ВЛИЯНИЕ МЕХАНОХИМИЧЕСКИ АКТИВИРОВАННОГО ДОКСОРУБИЦИНА И ОБЛУЧЕНИЯ С ЧАСТОТОЙ 40 МГц НА КЛЕТКИ КАРЦИНОМЫ ЛЕГКИХ ЧЕЛОВЕКА А–549

Цель: исследовать влияние механохимически активированного доксорубицина и электромагнитного облучения на клетки карциномы легких человека А-549. *Методы:* доксорубицин в твердой фазе механохимически активировали с интенсивностью подвода механической энергии 20 Вт/г. Опухолевые клетки подвергали электромагнитному облучению с частотой 40 МГц и с плотностью потока 2 Вт/см² при температуре 37 ℃. *Результаты:* частицы механохимически активированного доксорубицина имели размер в 10 раз меньше, чем официнальный доксорубицин; высокоэффективная жидкостная хроматография показала, что официнальный и механохимически активированный доксорубицин имеют одинаковые параметры. Механохимическая активация инициировала образование в препарате свободных радикалов с g-факторами $g = 2,005$, $g = 2,003$ и $g = 1,97$. LD_{50} для механохимически активированного доксорубицина была в 5 раз ниже, чем для официнального. Выживаемость клеток после воздействий уменьшалась в следующей последовательности: электромагнитное облучение → официнальный доксорубицин → механохимически активированный доксорубицин → официнальный доксорубицин с электромагнитным облучением → механохимически активированный доксорубицин с электромагнитным облучением. *Выводы:* воздействие механохимически активированного доксорубицина и препарата в комбинации с электромагнитным облучением при 37 ℃ показало более высокую эффективность действия на клетки карциномы легких человека А-549 по сравнению с официнальным доксорубицином.
Ключевые слова: клетки карциномы легких человека А-549, доксорубицин, механохимическая активация, электромагнитное облучение.